

Flow-Enhanced Epitaxial Ordering of Brush-Like Macromolecules on Graphite

Hui Xu,[†] Sergei S. Sheiko,^{*,†} David Shirvanyants,[†] Michael Rubinstein,[†]
Kathryn L. Beers,[‡] and Krzysztof Matyjaszewski[‡]

*Department of Chemistry, University of North Carolina at Chapel Hill, North Carolina 27599-3290, and
Department of Chemistry, Carnegie Mellon University, 4400 Fifth Avenue, Pittsburgh, Pennsylvania 15213*

Received August 8, 2005. In Final Form: October 7, 2005

Long-range orientational order in monolayers of brush-like macromolecules was achieved during spreading of a polymer melt on the surface of highly oriented pyrolytic graphite. The combination of wetting-induced flow and epitaxial adsorption of poly(*n*-butylacrylate) side chains on graphite led to the formation of large domains of uniaxially oriented rodlike molecules. The domain size varied from ca. 1 to 10 μm which is noticeably larger than the submicrometer-sized mosaic domains typically observed upon adsorption from solution. The increase in the degree of order is attributed to the flow-enhanced diffusion of the macromolecules within spreading monolayers which facilitates the epitaxial alignment of the large macromolecules. The diffusion coefficient was shown to increase linearly with the spreading rate. Even though the ordering occurred during flow, no correlation was observed between the molecular orientation and the flow direction. Thus, the role of the flow was not to induce the molecular orientation but to facilitate the intrinsic ordering process. This finding can inspire and lead to new strategies for constructing large scale ordered structures on surfaces.

1. Introduction

Thin films possessing long-range structural order on sub-100 nm length scales are vital for many technological applications such as magnetic recording¹ and optoelectronic² devices, molecular separation media,³ and liquid crystal displays.⁴ Ordered structures can be prepared using lithographic techniques^{5,6} and external fields.⁷ Ordering can also occur spontaneously upon adsorption of designed macromolecules (e.g., block copolymers)^{8–13} and colloidal particles.^{14–16} Self-organization of molecular and colloidal species can be further enhanced by specific interactions of the species with the underlying substrate through graphoepitaxy^{17–21} and surface epitaxy^{22–27} mechanisms.

Yet, the short-range order of the self-organized films precludes them from many applications because their domain size is usually no more than hundreds of nanometers. Ordering of molecules and colloidal particles on a surface is retarded by the 2D confinement and friction against the substrate. This particularly impacts larger species that experience severe steric hindrance and stronger interaction with the substrate. Such behavior is disadvantageous, since large macromolecules and particles are very attractive building blocks due to their native sub-100 nm size and a well-defined shape. Therefore, researchers are continuously looking for new mechanisms that would increase the degree of order in thin films. Here we report on the significant enhancement of epitaxial alignment of brush-like macromolecules achieved during spreading of the monolayer film on the surface of highly oriented-pyrolytic-graphite (HOPG). Unlike conventional flow-induced orientation of anisometric objects such as rodlike particles, liquid crystal molecules, and semi-flexible polymer chains,^{28–30} the observed molecular orientation is not coupled with the direction of flow. The role of the flow is merely to enhance diffusion and thus facilitate epitaxial ordering of the large macromolecules. These results were obtained using atomic force microscopy (AFM) which enabled real-time monitoring of the spreading process on the molecular scale.^{31,32}

* To whom correspondence should be addressed.

[†] University of North Carolina at Chapel Hill.

[‡] Carnegie Mellon University.

(1) Chou, S. Y.; Wei, M. S.; Krauss, P. R.; Fischer, P. B. *J. Appl. Phys.* **1994**, *76*, 6673.

(2) Li, R. R.; Dapkus, P. D.; Thompson, M. E.; Jeong, W. G.; Harrison, C.; Chaikin, P. M.; Register, R. A.; Adamson, D. H. *Appl. Phys. Lett.* **2000**, *76*, 1689.

(3) Volkmuth, W. D.; Austin, R. H. *Nature* **1992**, *358*, 600.

(4) O'Neill, M.; Kelly, S. M. *J. Phys. D -Appl. Phys.* **2000**, *33*, R67.

(5) Jain, K.; Zemel, M.; Klosner, M. *Proc. IEEE* **2002**, *90*, 1681.

(6) Wilbur, J. L.; Kumar, A.; Kim, E.; Whitesides, G. M. *Adv. Mater.* **1994**, *6*, 600.

(7) Schäffer, E.; Thurn-Albrecht, T.; Russell, T. P.; Steiner, U. *Nature* **2000**, *403*, 874.

(8) Morkved, T. L.; Lu, M.; Urbas, A. M.; Ehrichs, E. E.; Jaeger, H. M.; Mansky, P.; Russell, T. P. *Science* **1996**, *273*, 931.

(9) Huang, E.; Rockford, L.; Russell, T. P.; Hawker, C. J. *Nature* **1998**, *395*, 757.

(10) Bodycomb, J.; Funaki, Y.; Kimishima, K.; Hashimoto, T. *Macromolecules* **1999**, *32*, 2075.

(11) Thurn-Albrecht, T. et al. *Science* **2000**, *290*, 2126.

(12) Harrison, C.; Adamson, D. H.; Cheng, Z.; Sebastian, J. M.; Sethuraman, S.; Huse, D. A.; Register, R. A.; Chaikin, P. M. *Science* **2000**, *290*, 1558.

(13) Lopes, W. A.; Jaeger, H. M. *Nature* **2001**, *414*, 735.

(14) Denkov, N. D.; Velev, O. D.; Kralchevsky, P. A.; Ivanov, I. B.; Yoshimura H.; Nagayama K. *Nature* **1993**, *26*, 361.

(15) Micheletto, R.; Fukuda, H.; Ohtsu, M. *Langmuir* **1995**, *11*, 3333.

(16) Prevo, B. G.; Velev, O. D. *Langmuir* **2004**, *20*, 2099.

(17) Segalman, R. A.; Yokoyama, H.; Kramer, E. J. *Adv. Mater.* **2001**, *13*, 1152. Segalman, R. A.; Hexemer, A.; Kramer, E. J. *Phys. Rev. Lett.* **2003**, *91*, 196101. Segalman, R. A. *Mater. Sci. Eng., R: Reports* **2005**, *48*, 191.

(18) Hahn, J.; Webber, S. E. *Langmuir* **2004**, *20*, 1489.

(19) Sundrani, D.; Darling, S. B.; Sibener, S. J. *Langmuir* **2004**, *20*, 5091.

(20) Li, H.-W.; Huck, W. T. S. *Nanolett.* **2004**, *4*, 1633.

(21) Cheng, J. Y.; Mayes, A. M.; Ross, C. A. *Nature Mater.* **2004**, *3*, 823.

(22) Matthews, J. W. *Epitaxial Growth*; Matthews, J. W., Ed.; Academic Press: New York, 1975.

(23) Wittmann, J. C.; Lotz, B. *Prog. Polym. Sci.* **1990**, *15*, 909.

(24) Kim, S. O.; Solak, H. H.; Stoykovich, M. P.; Ferrier, N. J.; de Pablo, J. J.; Nealey, P. F. *Nature* **2003**, *424*, 411.

(25) Shchukin, V. A.; Ledentsov, N. N.; Bimberg, D. *Epitaxy of nanostructures*; Springer: Berlin, 2004.

(26) Rosa, C. D.; Park, C.; Thomas, E. L.; Lotz, B. *Nature* **2000**, *405*, 433.

(27) Severin, N.; Rabe, J. P.; Kurth, D. G. *J. Am. Chem. Soc.* **2004**, *126*, 3696.

(28) Keller, A.; Kolnaar, H. W. H. *Mater. Sci. Technol.* **1997**, *18*, 189.

(29) Maruyama, T.; Friedenber, M.; Fuller, G. G.; Frank, C. W.; Robertson, C. R.; Ferencz, A.; Wegner, G. *Thin Solid Films* **1996**, *273*, 76.

(30) Michalet, X.; Ekong, R.; Fougerousse, F.; Rousseaux, S.; Schurra, C.; Hornigold, N.; van Slegtenhorst, M.; Wolfe, J.; Povey, S.; Beckman, J. S.; Bensimon, A. *Science* **1997**, *277*, 1518.

(31) Xu, H.; Shirvanyants, D.; Beers, K.; Matyjaszewski, K.; Rubinstein, M.; Sheiko, S. S. *Phys. Rev. Lett.* **2004**, *93*, 206103.

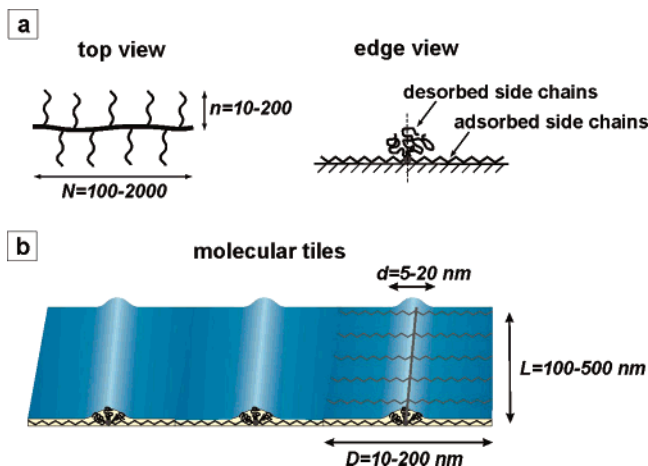


Figure 1. (a) Adsorption of brush-like macromolecules on surface results in partitioning of the side chains into two fractions: adsorbed and desorbed chains. Atom transfer radical polymerization allows precise control of the degree of polymerization of the backbone (N) and side chains (n) in a range of $N = 100\text{--}2000$ and $n = 10\text{--}200$, respectively. (b) The adsorbed molecular brushes can be viewed as miniature molecular tiles of a well-defined rectangular shape. Depending on the molecular dimensions, the length and width vary in a range of $L = 100\text{--}500$ nm and $D = 10\text{--}200$ nm, respectively, whereas the ridge of desorbed side chains is about $5\text{--}20$ nm in width and $1\text{--}5$ nm in height.

2. Molecular Tiles

Brush-like molecular architectures provide a powerful platform for construction of nanoscopic building blocks and devices.^{33–41} The size, shape, and physical properties of molecular brushes are well controlled by varying the length and grafting density of side chains.⁴² Additional structure-control mechanisms emerge upon adsorption of brush molecules on the surface. Figure 1a shows a schematic structure of a brush-like macromolecule adsorbed on a flat substrate, which divides the side chains into two fractions: adsorbed side chains and desorbed ones. One can view this as a miniature rectangular shaped tile with a ridge of desorbed side chains along the longitudinal axes of the tile (Figure 1b). The side chains play three important roles in controlling the shape and packing of these molecular tiles on surfaces. First, the steric repulsion between the adsorbed side chains stretches the backbone. Through variation of the side chain length and grafting density, one can tune the two-dimensional persistence length from 10 to 5000 nm. This length is from 0.2 to 100 times larger than the persistence length of DNA (~ 50 nm) and approaches that of F-actin ($\sim 10\ \mu\text{m}$) measured in solution. Second, adsorbed side chains separate the molecule's backbones. Depending on the side-chain length and the grafting density, the lateral size of the tile along with the intermolecular distance varies from 10 to 200 nm. Third, epitaxial adsorption of side chains onto a crystalline

substrate causes alignment of the backbone and thus results in remarkable enhancement of the ordering length-scale. As shown in Figure 1b, the surface-mediated alignment of the relatively short side chains induces orientational order of much longer polymer backbones. There is also a fourth role which is vital to our experiments. The ridge of the desorbed side chains provides the height contrast that allows identification and visualization of individual molecules by AFM.⁴³

3. Materials and Methods

Brush-like macromolecules consisting of polymethacrylate backbones and poly(n -butylacrylate) side chains were prepared by atom-transfer radical polymerization.^{44,45} This polymerization technique allows precise control of the degree of polymerization of the backbone (N) and side chains (n) in ranges of $N = 100\text{--}2000$ and $n = 10\text{--}200$, respectively (Figure 1a). In this work, we studied brushes with $N = 570 \pm 50$, $n = 50 \pm 5$. At room temperature, the polymer is a viscous liquid with a zero-shear viscosity $\eta_0 = 8340$ Pa·s and a glass transition temperature of $T_g \approx -50$ °C. The liquid nature of the material is essential as it allows for spontaneous spreading and molecular diffusion on surfaces.

We used three types of substrates: mica and two different grades of highly oriented pyrolytic graphite (HOPG). It is known that graphite induces epitaxial crystallization of alkanes and their derivatives due to close matching of the C–C–C length $l = 0.251$ nm and the crystallographic spacing of the HOPG lattice $a = 0.245$ nm.⁴⁶ Depending on the preparation conditions,⁴⁷ HOPG substrates may contain different types of surface defects including dislocations, grain boundaries, folds, and terraces. To examine the effect of the surface heterogeneity on the molecular ordering, we used two grades HOPG with different degrees of disorientation of the c -axis of monocrystalline mosaic blocks (Figure 2a): grade A with a mosaic spread of $0.4^\circ \pm 0.1^\circ$ and grade B with a mosaic spread $0.8^\circ \pm 0.2^\circ$. As such, HOPG grade A is a more oriented substrate with less defects per unit surface area.

Monomolecular films of the polymers were prepared on mica and graphite using two techniques: (i) spincoating from solution and (ii) spontaneous spreading of polymer melt. In the latter case, small drops of PBA brushes (volume ~ 1 nL, radius ~ 100 μm) were deposited onto the substrate and allowed to spread for several hours under a controlled environment (air, $T = 25$ °C, RH = 50%). For the spreading experiments on mica, an environmental chamber was used to maintain high relative humidity (RH) ranging from 90 to 99%. The prepared films were imaged by tapping mode AFM (Multimode Nanoscope IIIa, Veeco Metrology Group) using Si cantilevers (Mikromasch-USA) with a resonance frequency of about 140 kHz and a spring constant of about 5 N/m. The radius of the probe was measured to be less than 10 nm using a calibration standard.⁴⁸

Analysis of molecular dimensions and orientation was performed using a custom software program for analysis of digital images. The program is able to identify the molecular contour and determine the contour length, the curvature distribution, and the orientation of the molecular contour. To ensure accurate analysis of molecular properties, several images were collected in different areas of the same sample using different scan sizes and scan directions. For every sample, an ensemble of 300–500 molecules was analyzed to ensure appropriate averaging with a relative standard deviation below 10%.

4. Results and Discussion

4.1. Molecular Ordering. Panels a and b of Figure 3 show molecular organization of the films prepared by spincoating on

(32) Xu, H.; Shirvanyants, D.; Beers, K. L.; Matyjaszewski, K.; Dobrynin, A. V.; Rubinstein, M.; Sheiko, S. S. *Phys. Rev. Lett.* **2005**, *94*, 237801.

(33) Matyjaszewski, K.; Qin, S.; Boyce, J. R.; Shirvanyants, D.; Sheiko, S. S. *Macromolecules* **2003**, *36*, 1843.

(34) Cheng, G.; Boeker, A.; Zgang, M.; Krausch, G.; Müller, A. H. E. *Macromolecules* **2001**, *34*, 6883.

(35) Djalali, R.; Li, S.-Y.; Schmidt, M. *Macromolecules* **2002**, *35*, 4282.

(36) Schappacher, M.; Defieux, A. *Macromolecules* **2000**, *33*, 7371.

(37) Ikkala, O.; ten Brinke, G. *Chem. Comm.* **2004**, 2131.

(38) Mijović, J.; Sun, M.; Pejanović, S.; Mays, J. M. *Macromolecules* **2003**, *36*, 7640.

(39) Jha, S.; Dutta, S.; Bowden, N. B. *Macromolecules* **2004**, *37*, 4365.

(40) Percec, V.; Ahn, C.-H.; Ungar, G.; Yearley, D. J. P.; Möller, M.; Sheiko, S. S. *Nature* **1998**, *391*, 161.

(41) Zhang, A. F.; Barner, J.; Goessl, I.; Rabe, J. P.; Schluter, A. D. *Angew. Chem., Int. Ed.* **2004**, *43*, 5185.

(42) Sheiko, S. S.; Möller, M. *Chem. Rev.* **2001**, *101*, 4099.

(43) Sheiko, S. S.; Prokhorova, S. A.; Beers, K.; Matyjaszewski, K.; Potemkin, I. I.; Khokhlov, A. R.; Möller, M. *Macromolecules* **2001**, *34*, 8354.

(44) Matyjaszewski, K.; Xia, J. *Chem. Rev.* **2001**, *101*, 2921.

(45) Beers, K. L.; Gaynor, S. G.; Matyjaszewski, K.; Sheiko, S. S.; Möller, M. *Macromolecules* **1998**, *31*, 9413.

(46) Hooks, D. E.; Fritz, E.; Ward, M. D. *Adv. Mater.* **2001**, *13*, 227.

(47) Ohler, M.; Baruchet, J.; Galez, P. *J. Phys. D: Appl. Phys.* **1995**, *28*, A78.

(48) Sheiko, S. S.; Möller, M.; Reuvekamp, E. M. C. M.; Zandbergen, H. W. *Phys. Rev. B* **1993**, *48*, 5675.

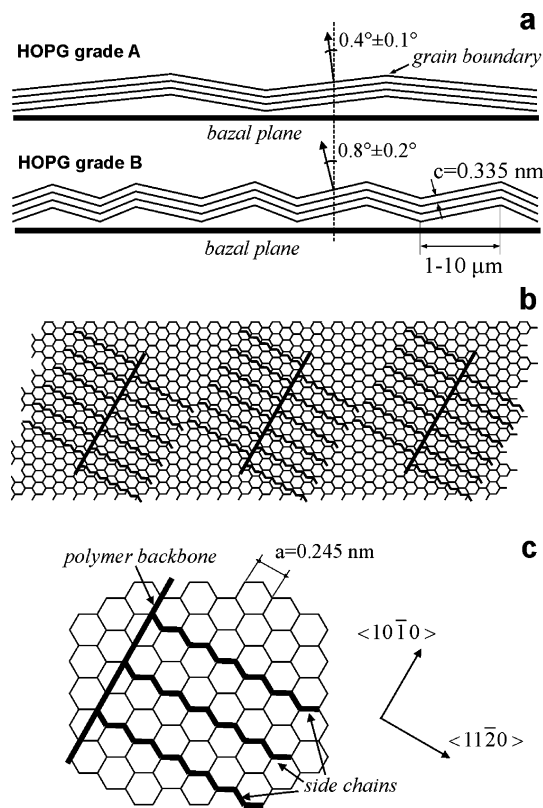


Figure 2. Schematic of the epitaxial adsorption of comblike molecules on graphite substrate: (a) HOPG substrates have a mosaic structure slightly disoriented mosaic blocks with a spread of the (0001) c axis of $0.4 \pm 0.1^\circ$ in grade A and $0.8 \pm 0.2^\circ$ in grade B; (b) Epitaxial adsorption of side chains leads to uniaxial alignment of polymer backbones along a particular crystallographic axis within the (0001) plane; (c) For example, if the side chains orient along the $\langle 11\bar{2}0 \rangle$ axis of the graphite lattice, this causes the backbone to orient along the $\langle 10\bar{1}0 \rangle$ axis.

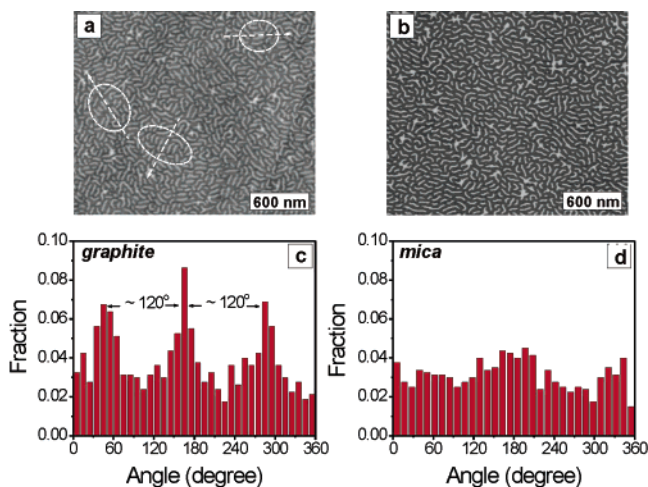


Figure 3. AFM was used to obtain height images showing molecular organization of spin-cast films of brush-like macromolecules on (a) graphite (grade A) and (b) mica substrates. The dashed circles and arrows in (a) highlight the ordered domains and their orientations; (c, d) angle distribution of molecules relative to the horizontal axis of the AFM images was measured on graphite and mica, respectively.

graphite and mica, respectively. The AFM height images show dense monolayers of wormlike macromolecules wherein the white threads correspond to the brush backbone and the area between the threads is covered by adsorbed side chains. Both on mica and graphite, the backbones of the adsorbed molecular brushes are almost fully extended showing the same value for a number

average contour length $L_n = 125 \pm 8 \text{ nm}$. This gives the average length per monomeric unit $l = L_n/N_n = 0.23 \pm 0.02 \text{ nm}$ which is close to the monomer length $l_0 \cong 0.25 \text{ nm}$ in the fully extended all-trans conformation of the aliphatic backbone. In these images, one can also see small domains of uniaxially aligned molecules highlighted by dashed circles. The lateral size of the domains ranges from 100 to 600 nm with no visible indications of long-range molecular order. However, closer examination of the film structure on graphite (Figure 3a) reveals preferential orientation of the molecules along three axes as demonstrated by three distinct peaks in the angle distribution of molecular orientation (Figure 3c). The angle difference between the three peaks is approximately 120° , which is consistent with the 3-fold symmetry of the graphite (0001) surface.⁴⁹ In contrast, crystalline mica does not show any particular orientation (Figure 3b) resulting in random distribution of the angles (Figure 3d).

The orientational order of the brush-like macromolecules on the graphite drawn in Figure 2b is attributed to the well-known epitaxial adsorption of alkyl side chains on graphite along one of the three crystallographic axes of the (0001) surface.^{50–52} For example, this leads to alignment of the side chains along the $\langle 11\bar{2}0 \rangle$ axis of the graphite lattice which in turn causes the backbone to orient along the $\langle 10\bar{1}0 \rangle$ axis (Figure 2c). The lack of such ordering on the mica surface is ascribed to a spatial mismatch between the mica lattice and molecular architecture. The disordered structure on mica could also be attributed to the thin layer of water that condensed from the surrounding atmosphere onto the hydrophilic surface of mica.⁵³ The water layer distorts epitaxial interactions between the crystalline mica and pBA side chains. Note that changing preparation conditions, such as annealing time, temperature, and solution concentration, did not improve molecular ordering either on graphite or mica substrates. Seemingly, thermal diffusion of the large macromolecules within dense monolayers is prohibitively slow and hinders the ordering process.

To enhance molecular motion, thin films were prepared by a different method: spreading of a polymer melt on a solid substrate. For this purpose, we deposited a drop of the pBA brush melt to a solid substrate (mica or graphite) and monitored the spreading process by AFM. Both substrates cause spontaneous spreading of the melt resulting in a monolayer-thick precursor film which advances ahead of the macroscopic drop.^{54–56} The spreading rate depends on the substrate type due to the friction between the monolayer and substrate, which in turn directly affects the length of the precursor film. It took about 10 h for the film spreading on graphite to achieve a sizable length of $10 \mu\text{m}$ while the same length on mica at a relative humidity of 95% was achieved within 10 min. The relatively slow motion on graphite allowed in situ observation of the molecular structure of the precursor film,³¹ whereas on mica, we performed ex-situ measurements after the spreading process was halted by reducing the relative humidity from 95% to 50%.

Figure 4 shows typical images of precursor films obtained on mica and graphite (grade A) surfaces, respectively. The contrast between the two images is significant. On graphite, the molecules

(49) Wu, N. J.; Ignatiev, A. *Phys. Rev. B* **1982**, *25*, 2983.

(50) Bauerle, P.; Fisher, T.; Bidlingmeier, B.; Stabel, A.; Rabe, J. P. *Angew. Chem., Int. Ed.* **1995**, *34*, 303.

(51) Prokhorova, S. A.; Sheiko, S. S.; Mourran, A.; Möller, M.; Beginn, U.; Zipp, G.; Ahn, C.-H.; Percec, V. *Langmuir* **2000**, *16*, 6862.

(52) Severin, N.; Rabe, J. P.; Kurth, D. G. *J. Am. Chem. Soc.* **2004**, *126*, 3696.

(53) Hu, J.; Xiao, X.-D.; Ogletree, D. F.; Salmeron, M. *Science* **1995**, *268*, 267.

(54) De Gennes, P. G. *Rev. Mod. Phys.* **1985**, *57*, 827.

(55) Hardy, W. B. *Philos. Mag.* **1919**, *38*, 49.

(56) Heslot, F.; Fraysse, N.; Cazabat, A. M. *Nature* **1989**, *338*, 640.

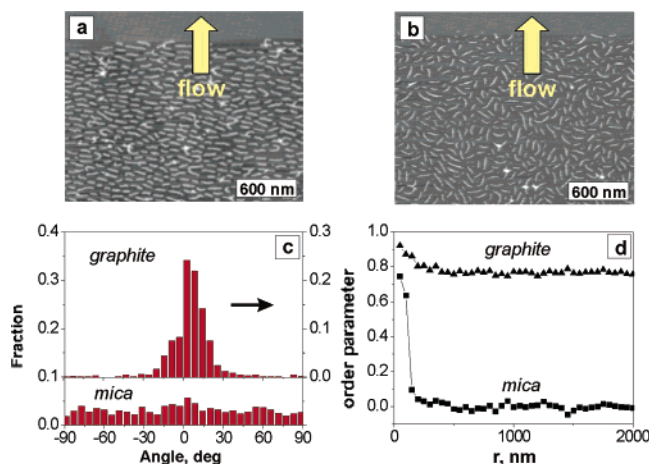


Figure 4. Precursor films prepared from spontaneous spreading of the comblike molecules on (a) graphite (grade A) and (b) mica. (c) On graphite, molecules show a narrow angle distribution measured relative to the horizontal axis. In contrast, molecules on mica reveal a broad (isotropic) angle distribution. (d) While the two-dimensional orientational order parameter $S = 2\langle \cos^2 \theta \rangle - 1$ levels off on graphite at $S = 0.75$; it rapidly drops to zero on mica.

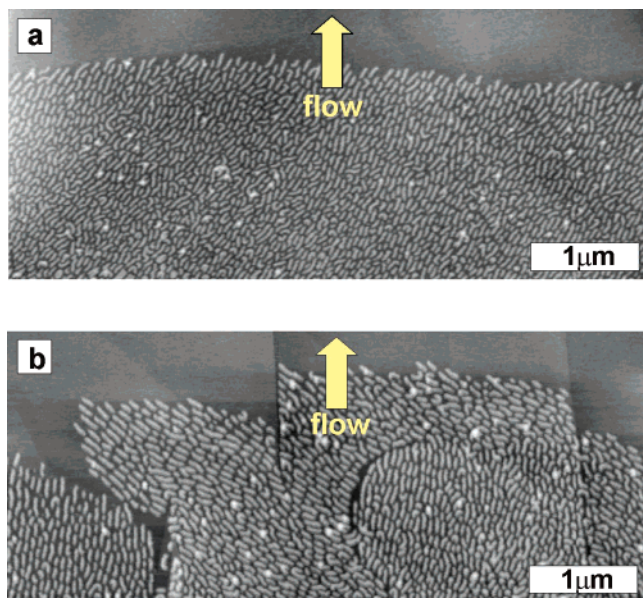


Figure 5. Two large-scale AFM height images demonstrate examples of different molecular organization within the flowing precursor film on graphite (grade A). Panel a shows a large domain of uniaxially oriented molecules, whereas panel b reveals a multidomain structure.

are all aligned along a single direction (Figure 4a) as evidenced by a narrow angle distribution (Figure 4c). In stark contrast, the molecules on mica (Figure 4b) are completely disordered resulting in a broad distribution of angles (Figure 4c). The degree of order was analyzed using the orientational order parameter $S = 2\langle \cos^2 \theta \rangle - 1$ for two-dimensional systems, where θ is defined as the angle between each molecule and a certain director (horizontal axis in this case). As shown in Figure 4d, the film on graphite is characterized by a slight decay of the order parameter at short distances which then levels off at $S \approx 0.75$. In contrast, the order parameter on mica rapidly drops to $S \approx 0$ already at 100 nm, i.e., intermolecular distance, indicating a complete lack of correlation between orientations of neighboring molecules.

Next, we show that the molecular orientation does not depend on the flow direction. Figure 5 shows two large-scale images that give an overview of the molecular arrangement in the spreading film. Depending on the structure (perfection) of the

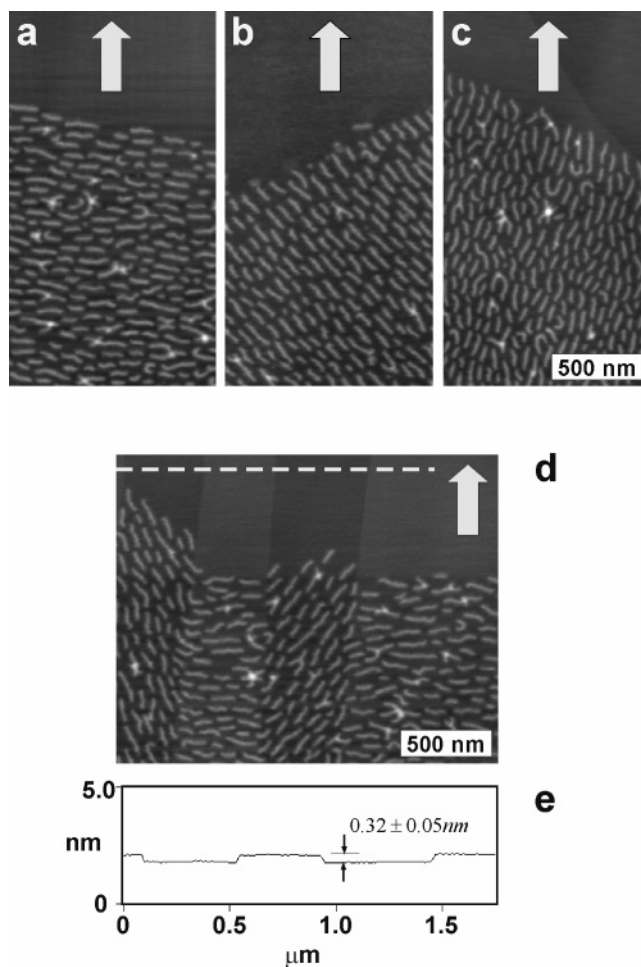


Figure 6. (a–d) Higher magnification height images were measured in different areas of the precursor film on graphite. The images reveal a lack of correlation between the flow direction and orientation of the flowing molecules. This behavior is clearly seen in (d) showing differently oriented domains in the same area of the precursor film. (e) From the cross-sectional profile along the dashed line in (d), one determines a terrace thickness of 0.32 ± 0.05 nm which matches with the AB interlayer spacing $c = 0.335$ nm of HOPG (see Figure 2a).

substrate, one can either observe a large domain of molecules aligned along a single direction (Figure 5a) or a mosaic of smaller domains with differently oriented molecules (Figure 5b). Figure 6a–c shows three higher resolution images that are captured in different areas of the precursor film in order to demonstrate different orientations of the molecules with respect to the flow direction. The domains are visibly confined by terraces and other surface defects of the HOPG substrate. For example, the AFM image in Figure 6d reveals three different molecular orientations in an area of the HOPG substrate that contains several monomolecular terraces of graphite next to each other. The monomolecular origin of the terraces was confirmed with the cross-sectional profile in Figure 6e giving a step height of 0.32 ± 0.05 nm which matches with the AB interlayer spacing $c = 0.335$ nm of HOPG.⁴⁹ Note that the terraces in Figure 6d form native trenches or flow channels wherein molecules demonstrate different flow rates. However, we do not have enough evidences to explain the difference in flow rates, which may be due to channel confinement or to variation in friction at the substrate as expected from differently oriented molecules. This unusual flow behavior is currently under investigation.

From the AFM images one can conclude that the alignment of brush molecules is solely determined by the crystallographic

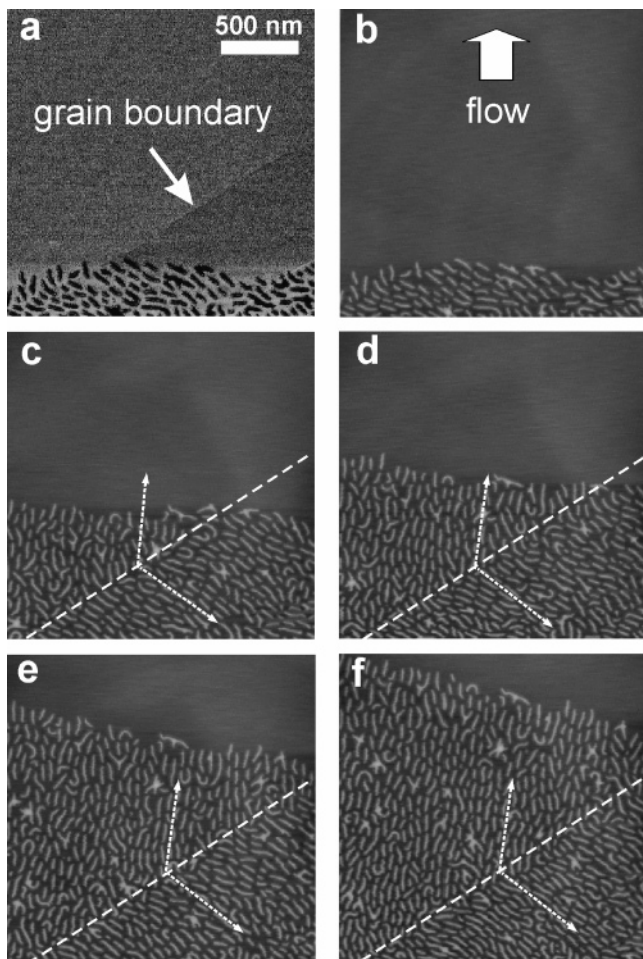


Figure 7. AFM was used for real-time imaging of the shift in molecular orientation upon crossing a grain boundary during spreading of pBA brushes on graphite (grade A). The micrographs (a) and (b) represent phase and height AFM images that are taken from the same sample area in order to visualize the grain boundary between two mosaic blocks (Figure 2a). The grain boundary shows no height contrast and becomes visible only in the phase image (white arrow). Then white dashed lines were used to highlight the grain boundary in the subsequent height images from (b) to (f). The dotted lines in images (b–f) indicate the average molecular orientation within the two domains. The angle between the directors was measured to be about 120° .

lattice of the underlying substrate and independent of the flow direction. The substrate-controlled molecular orientation was confirmed by in situ monitoring of the flow process on HOPG where molecules change their orientation upon displacement over a grain boundary (Figure 7). The boundary, clearly seen in the phase image in Figure 7a (marked by the white arrow), is undetectable in the topographic image in Figure 7b suggesting that there is virtually no height difference between the two monocrystalline grains or mosaic blocks (see schematics in Figure 2a). The in situ monitoring of the flow process in this area by AFM enabled unique observation of how individual molecules abruptly shift their orientation, one molecule at a time, after crossing the grain boundary to join a new domain with a 120° -turned molecular orientation. The sharp interface between the two domains of differently oriented brush molecules exactly coincides with the grain boundary of the substrate marked by the dashed line in Figure 7c–f.

4.2. Flow Enhanced Molecular Diffusion. The lack of correlation between the flow direction and the molecular orientation is consistent with the recently confirmed plug-flow

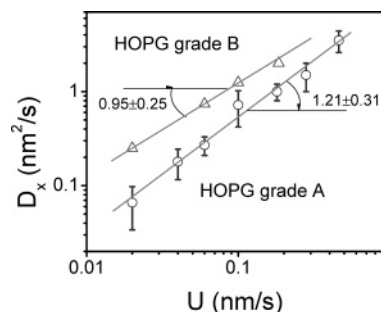


Figure 8. Diffusion coefficients were measured on two HOPG substrates (grade A and grade B) as a function of film spreading rate. Only the x -component of the diffusion coefficient (D_x), i.e., the diffusion in perpendicular to the flow direction, was considered to rule out the possible effects of convective diffusion. Both substrates show nearly linear increase of the diffusion coefficient with spreading rate. The lesser oriented HOPG grade B substrate shows greater diffusion than of the more oriented HOPG grade A.

mechanism of the mass transport in spreading monolayers of polymer brushes.³¹ Unlike shear-flow, the plug-flow mechanism⁵⁷ assumes that all species move with the same velocity, i.e., with no velocity gradient which is typically responsible for the orientation of anisometric molecules and particles. Therefore, there must be another mechanism of epitaxial ordering of brush-like macromolecules associated with the flow.

Molecular epitaxy is a thermodynamic process wherein the molecules arrange themselves on the substrate lattice in order to minimize the free energy of the system.⁴⁶ Typically, in-plane diffusive translational and rotational motions facilitate molecular ordering in monomolecular films. However, the thermal energy is usually weak compared to the strong molecule–substrate interactions of about kT per contact between monomeric unit and substrate. Therefore, long-range ordering may not be easily achieved or takes an extremely long time. This was evidenced by the lack of long-range order in the spincast films (Figure 3a) even after 20 h annealing at $T = 95^\circ\text{C}$ which is 150°C above the bulk glass transition temperature of pBA. However, mobility of surface-confined molecules may be enhanced by flow. Figure 8 shows that the diffusion coefficient of brush-like macromolecules within the flowing monolayer increases linearly with the flow rate. This observation on the HOPG-grade A surface confirms the previously reported linear increase of molecular diffusion on the HOPG-grade B substrate.³¹ Unlike the thermal diffusion in static films, the diffusion in spreading monolayers is attributed to the flow-induced molecular diffusion. The enhanced diffusion leads to an increase in the effective kinetic energy of the molecules and thus explains why the epitaxial ordering of brush molecules was drastically expedited despite the strong molecule–substrate interactions. This is analogous to effective temperature for granular materials,⁵⁸ which could be up to 100 times higher than ambient temperature.

4.3. Effect of HOPG Quality (Grade A versus Grade B). Here we compare molecular ordering and dynamics within spreading monolayers on two types of graphite substrates with different degrees of mosaic disordering. As discussed above, spreading monolayer on HOPG grade A substrate demonstrates an order parameter of 0.75 which persists over long distances beyond $10\ \mu\text{m}$ (Figure 4d). A different behavior was observed on the HOPG grade B substrate. As shown in Figure 9, the orientation order parameter rapidly decays to zero at a low correlation length of 390 nm (about 8 intermolecular distances).

(57) Brochard, F.; de Gennes, P. G. *Phys. Lett.* **1984**, *45*, L597.

(58) Ono, I. K.; O'Hern, C. S.; Durian, D. J.; Langer, S. A.; Liu, A. J.; Nagel, S. R. *Phys. Rev. Lett.* **2002**, *89*, 095703.

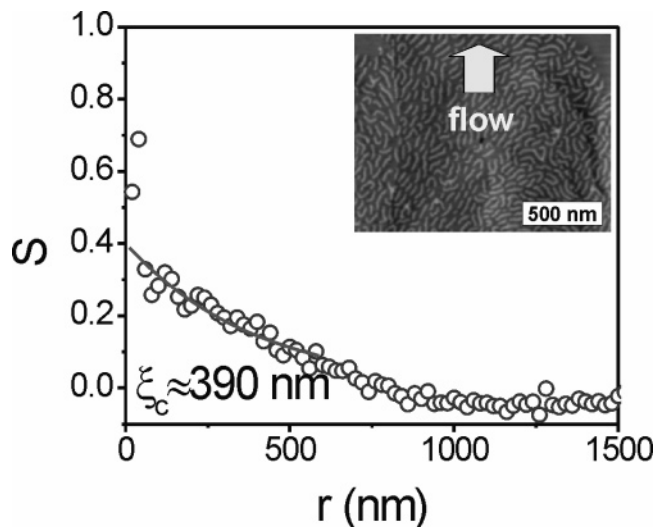


Figure 9. Orientation order parameter $S = 2\langle \cos^2 \theta \rangle - 1$ was measured as a function of intermolecular distance for a spreading monolayer of pBA brushes on HOPG grade B substrate. The inset shows a typical AFM height image of a spreading monolayer on a HOPG grade B substrate. The order parameter demonstrates an exponential decay with a correlation length of 390 nm.

In addition, the film on the more uniform HOPG grade A was shown to spread almost two times faster than on the HOPG

grade B. The difference in spreading rate can be attributed to the difference in concentration of surface defects and to the more coherent motion of molecules due to long-range ordering. As shown in Figure 8, the molecular diffusion coefficient is noticeably smaller on HOPG-A than on HOPG-B.³¹

5. Conclusions

In summary, we have demonstrated that flow facilitated the epitaxial ordering of brush-like macromolecules on graphite, resulting in a long-range orientational order. The brush-like architecture leads to a length-scale enhancement effect as the epitaxial adsorption of the short side chains causes alignment of giant macromolecules. The increase in the degree of orientational order is attributed to the flow-enhanced diffusion of molecules, which enables them to find an energetically favorable arrangement. Our findings suggest that convective flow is more efficient than thermal motion in improving ordering of large molecular and colloidal species. This may result in new techniques for fabricating long-range ordered structures on surface.

Acknowledgment. This research program was supported by the National Science Foundation (ECS 0103307 and DMR 0306787). M.R. acknowledges financial support from NASA under agreement NCC-1-02037.

LA052163C